Simulation of Saturn V S-II Stage Propellant Feedline Dynamics

R. S. RYAN,* L. A. KIEFLING,† AND H. J. BUCHANAN‡
NASA Marshall Space Flight Center, Huntsville, Ala.

AND

W. A. JARVINEN§
Northrop Corporation, Huntsville, Ala.

Oscillations involving the propellant feedlines, engines, and longitudinal structural modes of the Saturn V S-II stage are investigated, using an electronic analog computer. The methods used to develop mathematical models and some problems encountered are described. The effect of a nonlinear gas bubble (cavitation) at the pump inlet is studied. The simulation was able to match several characteristics of the flight, including stability variations with NPSH, amplitude sensitivity, and nonlinear waveforms. The cause of the limit cycle which occurred on two flights was not found. The need exists for accurate and complete test data, especially for structural damping and local and engine dynamics.

Nomenclature

CECO = center engine cutoff
f_1, f_2, f_2 = frequency constants
F = engine thrust
NPSH = net positive suction head
p = pressure
p_{os} = LOX suction pressure
V = volume
γ = ratio of specific heats c_p/c_v for a gas
ζ = damping constant

Introduction

POGO is a closed-loop oscillation involving longitudinal structural vibrations and pressure oscillations within the liquid rocket propulsion system. The theory of such oscillations is now well understood and are probably best described by Rubin.[1] However, the detailed problem of obtaining accurate data for a complex system over a wide range of operating conditions remains.

The oscillation that occurs during the S-II stage is not a typical POGO oscillation in that it is highly localized and includes basically the engines, cross-beam engine mount, propulsion lines, and LOX bulkhead. The fact that the over-all vehicle longitudinal modes are not participating presents a real modeling problem since only the higher-ordered localized modes are participating in the oscillation. Also, the oscillations observed in flight were nonlinear, a fact which further complicates the mathematical modeling and analysis prediction of flight response. This paper presents a nonlinear time-varying model of the S-II POGO phenomenon and compares results with the flight.

Three basic disciplines are involved in achieving good models: 1) methods of evaluating system or subsystem characteristics, 2) component modeling, and 3) system modeling. Each discipline contains the same basic procedure. Step 1 requires the engineer to formulate some understanding or explanation of the physical phenomenon observed or expected. Step 2 is a collection of data to support these assumptions. Step 3 constructs a model to match the theorized physical phenomenon. This model is usually of an analytical nature, but it can be a combination of analytical and numerical form. Step 4 is the analysis which, in general, will point up weaknesses and strong points in the theorized explanation, thus requiring the process to be repeated through all steps until an adequate model results. A tendency to bypass steps or shift loops will generally lead to inaccurate results, wasted time, and frustration.

The procedure for properly describing the connecting interfaces between components when assembling the system model is conceptually sound but not always straightforward. The preferred approach is to model analytically the subsystem or system, using tests to verify or update the model. In certain instances, analytical representations are impractical or impossible, and test data must be used in the system simulation. Great care must be exercised in the direct use of the test data in analysis. Two problems are as follows: 1) curve fits or extrapolation of data can introduce mathematical instabilities that do not exist physically; and 2) test data contain effects of test facilities and instrumentation, ill-defined interfaces, or other components that are not easily identifiable.

The basic information needed for each subsystem includes 1) the describing equations, 2) the coefficients of equations or fits (input data), time-varying effects etc., 3) the simplification that is possible, the assumption, limitations, data spreads etc., 4) frequency response (gain and phase), and 5) nonlinearities. A typical POGO analysis involves four subsystems: structure, feedlines, pumps, and devices for eliminating POGO (fixes).

The theoretical analysis must correlate 1) the time response of the system to disturbances or initial conditions, 2) frequency responses of the system (when practical), and 3) stability analysis of the system to predict onset and decay of instabilities and the magnitude of the stability or instability of the system (stability margins). (Item 3, as a general rule, is applicable only to linear systems.) The time response is necessary to predict oscillation amplitudes, and is very helpful, if not necessary, for understanding nonlinear behavior characteristics. Also, the effect of time-varying vehicle characteristics can be fully understood and interpreted only by the use of time-response techniques. In this paper, emphasis is placed on the time-response simulation approach.

Presented as Paper 70-626 at the AIAA 6th Propulsion Joint Specialist Conference, San Diego, Calif., June 15–19, 1970; submitted June 23, 1970; revision received September 23, 1970. The authors gratefully acknowledge the assistance from the many persons who have contributed to this work, especially those of the MSFC Astronautics Laboratory and North American Rockwell Corporation.

* Deputy Chief, Dynamics and Control Division. Associate Fellow AIAA.
† Chief, Structural Dynamics Section. Member AIAA.
‡ Chief, Analytical Investigation Section. Member AIAA.
§ Aerospace Engineer, Electro-Mechanical Division.

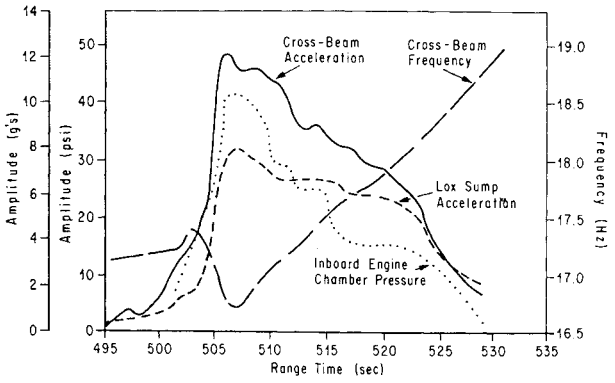

Fig. 1 AS-504 flight data.

Flight Test Results

POGO oscillations during S-II stage powered flight have been observed during several flights. Some of the data from the AS-504 vehicle are presented in Fig. 1, which shows a shift in structural and propulsion system frequency occurs at approximately 500 sec. The accelerations of the cross-beam (which supports the center engine) and the LOX pump, and the center engine's chamber pressure all peak at this time. All of the amplitudes subsequently fall back toward zero, and by 530 sec the oscillations are back to their normal steady-state level. It was these rather significant oscillations which prompted the early CECO and initiated this attempt to model the phenomenon.

The Apollo 13 flight AS-508 had an even more severe POGO oscillation. The oscillation occurred much earlier in flight and reached such large acceleration amplitudes (cross-beam acceleration at center engine of 33 g's) that large pressure fluctuations occurred triggering a pressure switch, shutting off the engine after only 160 sec of the S-II burn. ECO at this time was approaching the earliest time at which cutoff could have occurred and the mission still be achieved. Figure 2 shows the cross-beam acceleration and LOX pump inlet pressure during the large amplitude oscillations. Observe the nonlinearity in the LOX inlet pressure oscillation curve. This curve has very sharp peaks and flat or round bottoms, and there is a harmonic present that is shifting downward with increasing amplitude.

Structure

Development of an adequate structural model has been a major problem. The first four modes of the S-II LOX tank aft bulkhead have been found to be significant, and until recent months, no attempts had been made to represent these higher modes. The modeling of the S-IVB LOX tank is also very critical because it has a large mass and a natural frequency near the POGO frequency, and it can therefore significantly affect the generalized mass and structural gains. Development of a structural model using data from dynamic

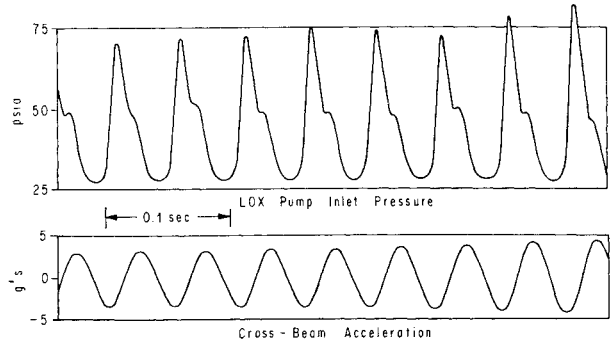

Fig. 2 AS-508 flight response.

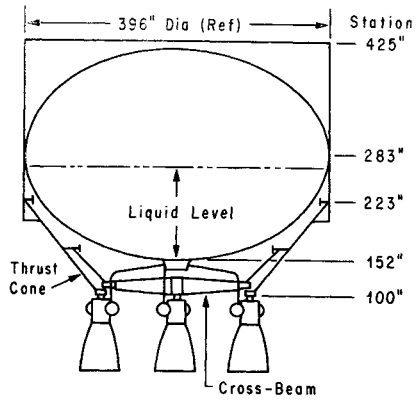

Fig. 3 S-II aft structure configuration.

tests of the total vehicle, flight data, and bulkhead ground tests was not very successful.

The aft structure S-II configuration is shown in Fig. 3. The four outboard engines are mounted on the thrust cone, and the center engine is mounted on a cross-beam which is pinned at the ends. For some modes of the vehicle, such as those from the dynamic test shown in Fig. 4, the kinetic energy is concentrated in the cross-beam area. The testing of the aft structure is complicated by an apparent effect of the static forces on the dynamic characteristics. Dynamic and static influence coefficients do not compare well, and combined testing is not practical. State-of-the-art improvement is needed to predict structural damping for components of this type. These deficiencies make accurate modeling of the over-all structural model difficult.

Frequencies from ground tests of an S-II LOX tank are shown in Fig. 5. Three bulkhead frequencies cross the thrust structure frequency, further complicating the over-all structural modeling. The highest propellant level tested was only slightly above the tank equator, and flight data indicate that the fourth bulkhead mode also crosses the thrust structure frequency.

The structural modes used were calculated by the Space Division of North American Rockwell. Structural damping of 1.5% of critical, which was used for system calculations, was determined from ground tests of the LOX tank and thrust structure.

Feedlines

As shown in Fig. 6a, the fluid and wall are normally divided into segments for analytical purposes. For the case under consideration, the S-II center LOX line, the fluid compressibility, and line elasticity may be neglected without any great effect on the first line mode since these stiffnesses are much

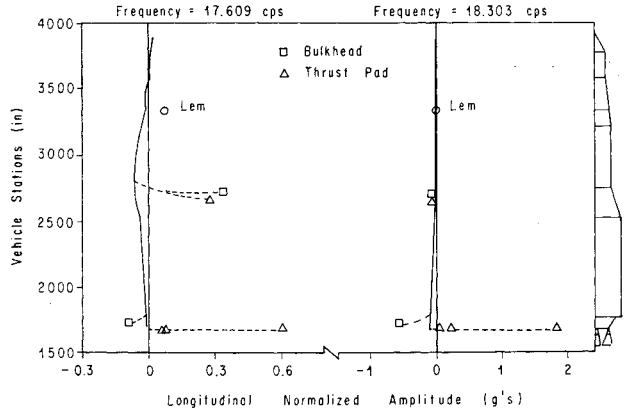

Fig. 4 Dynamic test mode shapes.

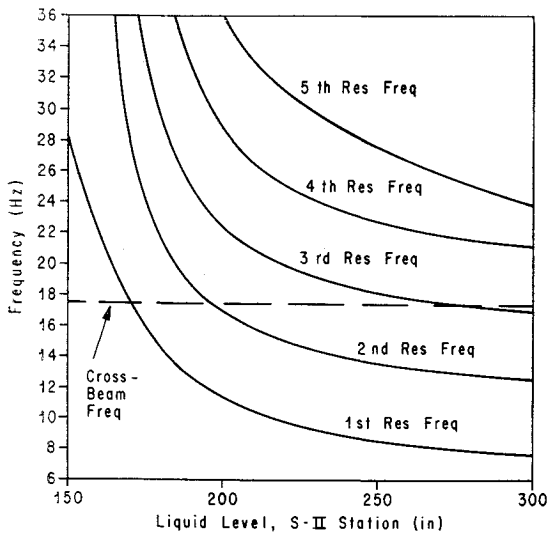

Fig. 5 S-II aft LOX bulkhead resonant frequencies.

greater than the stiffness of the combined cavitation bubble and pump inlet impedance. The system can therefore be modeled as shown in Fig. 6b, with the mass representing the actual fluid mass in the line. The system must be separated at the line pump interface because the acceleration at this point is a forcing function on the line, but not on the pump.

Each of the J-2 engines is fed from the LOX pump by an 8-in.-nominal-diam. line. Line lengths are 53 in. for the inboard line and 110 in. for the outboard line. However, the effective length of the center line is less due to a diameter increase at the elbow. Because of the difficulty of analytically modeling the line compliance, tests were needed to determine this compliance. Typical results from the initial attempt to measure the dynamic properties of the center feedline are shown by the solid curves in Fig. 7. A good resonance was obtained, and it was possible to model the dynamics using a two-degree-of-freedom damped spring-mass model. The values of C and K, damper and spring constant, can be used, along with a mass value for the flight line alone as one model for the line system.

In the next attempt to measure the line dynamic characteristics, a gas accumulator was installed near the juncture of the flight and test facility lines. Typical results are shown by the dashed curves in Fig. 7. The static pressure and PU valve position are unchanged from those of the previous figure.

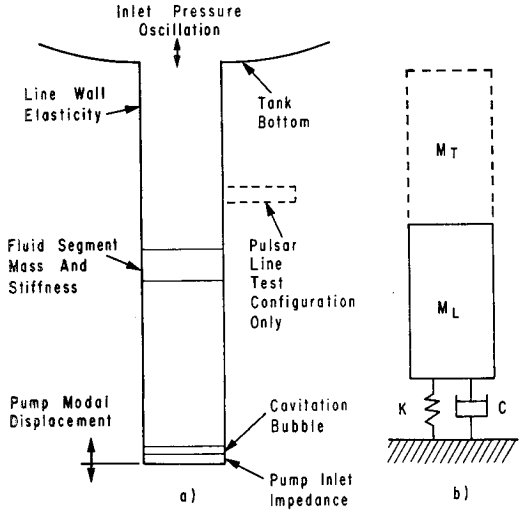

Fig. 6 Significant feedline parameters and feedline spring mass model.

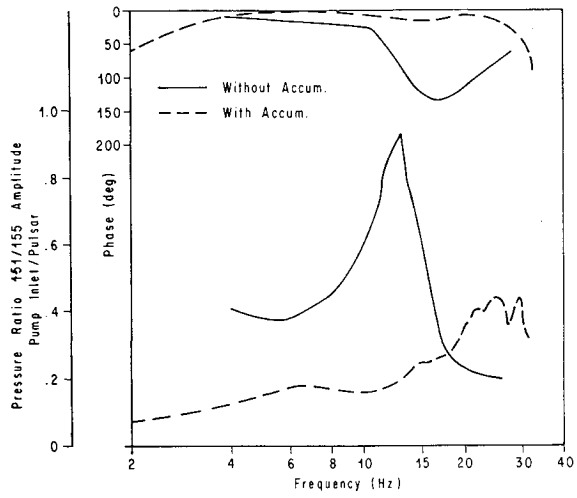

Fig. 7 Pressure ratio response.

Here, for reasons not understood, a clear resonance does not exist.

All S-II flights which have exhibited POGO have shown a distinct nonlinearity in the propulsion loop. This nonlinearity does not occur in the structure with all structural responses showing definite linear characteristics. The hypothesis used in this analysis for the nonlinearity of the propulsion system loop is that the bubbles just forward of the pump act as a gas spring, controlling or producing the frequency of the feedline. If it is first assumed that the bubbles can be lumped into one bubble (for convenience), the spring constant of that bubble is highly nonlinear from pressure volume considerations. This can be formulated in terms of adiabatic conditions as $pV^\gamma = p_0V_0^\gamma$ = constant. We know, however, that the number of bubbles is not constant. Since this flow is of a cryogenic fluid under oscillatory forces (pump mounting), vapor is changed to liquid and liquid to vapor. Also, there is a spring in series with this bubble which is composed of the fluid compressibility and line elasticity. The real instantaneous pressure force at the pump is therefore the combination of all these phenomena. An attempt was made, based on these observed test data, to construct a reasonable representation of this force, which is shown on Fig. 8 as a spring-mass ratio (K/M_L in Fig. 6b) vs NPSH (pressure). Allowing the spring force to vary as an instantaneous function of the pressure produces the nonlinearity desired. The test and flight, previously discussed, were used to establish the frequency for the operating point around 42 NPSH and the upper asymptote. The greatest unknown is at the lower end of the curve where test data are not available. Although this nonlinear approach has not been completely verified, its use appears valid from general observations of POGO in actual vehicle flights.

Some insight into the absence of a clear resonance and problems of measuring line frequencies in test can be gained

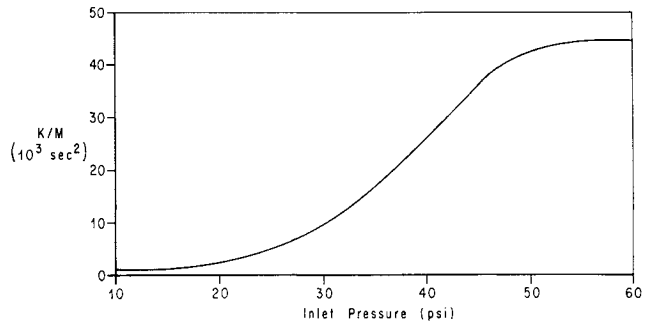

Fig. 8 Nonlinear spring constant for LOX pump cavitation bubble.

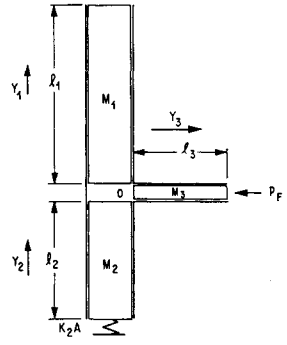

Fig. 9 LOX line model with pulsar.

by studying a representative undamped system (see Fig. 9), which consists of three rigid masses and a spring. The first mass represents the fluid in the line above the pulsar line; the second, the fluid below the pulsar line; and the third, the fluid in the pulsar line. The inlet is represented by A and the pulsar line area by A/q. Point O is a reference point with pressure p_o, which acts equally on all adjoining faces. (Nonlinear studies have shown this to be a good assumption for the actual amplitudes involved.) P_f is the pulsar pressure; y_i represents the displacements of the ith mass, $i = 1, 2, 3$; and ρ is the fluid density. The cavitation bubble and pump inlet impedance are combined into a pressure spring K_2.

Case 1: Consider y_3 and y_4 fixed. If a sinusoidal oscillation is assumed, then the equation for the resonant frequency of the fluid in the line must be

$$\omega^2 = K_2/\rho(l_1 + l_2) \tag{1}$$

Case 2: Consider a free-body diagram of the second mass m_2. The forces are: a) a spring force on the bottom $F_k = -K_2 y_2 A$; b) an inertia force $F_i = \omega^2 \rho l_2 y_2 A$; and c) a pressure force $F_f = -p_0 A$.
The sum of these must then be zero:

$$(K_2 - \omega^2 \rho l_2) y_2 - p_o = 0 \tag{2}$$

The resonant frequency of the ratio p_{os}/p_o (or y_2/p_0) is thus seen to be different from the resonance of the total system.

Case 3: To find the effect of the pulsar line on the resonant frequency, the following system of equations may be solved:

$$\ddot{y}_1 l_1 \rho A = p_0 A \tag{3}$$

$$\ddot{y}_2 l_2 \rho A + K_2 A y_2 = -p_0 A \tag{4}$$

$$\ddot{y}_3 l_3 \rho A/q = p_0 A/q - p_f A/q \tag{5}$$

$$\ddot{y}_3 = (\ddot{y}_2 - \ddot{y}_1) q \tag{6}$$

The first three equations are from force summations, and the fourth is a continuity equation. Pressure is assumed equal

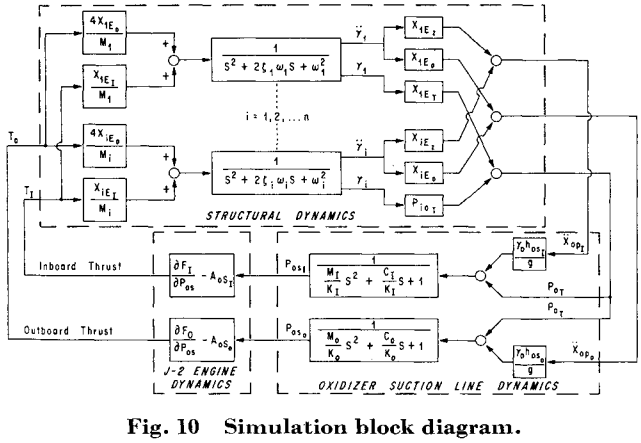

Fig. 10 Simulation block diagram.

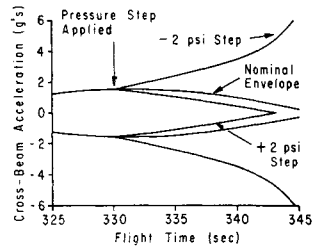

Fig. 11 Effect of ullage pressure on stability.

on all three faces. Elimination of the variables gives

$$\left[K_2 - \omega^2 \rho\left(l_2 + \frac{l_1}{1 + l_1/l_3 q}\right)\right] y_2 = p_f \frac{l_1/l_3 q}{1 + l_1/l_3} \tag{7}$$

This equation will have the same resonance as case 2 for $l_3 = 0$ and the same resonance as case 1 as l_3 and q become large. The conclusion to be drawn from this simple model study is that the test setup introduces multiple resonances in the feedline.

Line parameters from telemetered flight measurements are now being used in the system studies. The S-II amplitudes were low but detectable by the use of statistical data reduction techniques, thus giving credence to the assumed line frequency between 25 and 28 Hz.

Engine Characteristics

The J-2 engine responds to the dynamic pressure in the feedline and produces thrust oscillations which excite the vehicle structure, thus sustaining the longitudinal vibrations. For use in modeling the POGO phenomenon, an engine transfer function relates the thrust to the fuel and oxidizer supply pressure and flow rate. For the present state-of-the-art, such an expression can only be arrived at empirically. However, a study of existing theory is valuable in understanding the physical problem and reducing it to a usable model.

This problem can be divided by disciplines into two parts. The combustion chamber and nozzle can be modeled using the techniques of thermodynamics and chemical kinetics. However, since a great deal of experimental data is available and indicates this part of the problem to be relatively straightforward, most investigators have been content to use an empirical expression relating thrust to chamber pressure. The other half of the system is quite another problem. Pumps and turbines, having been studied extensively, are well understood. However, cavitation which is of primary importance, cannot be treated with such a simple model.

Cryogenic propellants at very near their saturation conditions are passed through the pump at very high velocities. This naturally results in regions of low pressure and cavitation. This cavitation bubble figures strongly in the dynamics of the entire fluid loop. Various investigators have attempted to analytically treat the pump including the bubble,[2,3] but because the bubble is very much dependent upon local conditions within the pump, no really adequate solution is available.

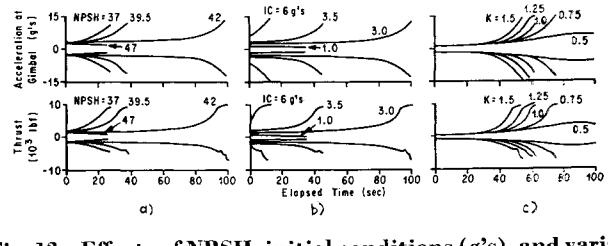

Fig. 12 Effects of NPSH, initial conditions (g's), and variations in nonlinearity on system response at 210-sec S-II burn time.

In the present simulation an empirically derived transfer function was used. For simulation purposes, it was found useful to consider all of the vapor volume as a single bubble and to imagine it to be located just ahead of the pump at the interface between the feedline and the pump.

The problem of measuring the input and output across the pump and determining a transfer function for the system was complicated by the mechanics of the physical arrangement.

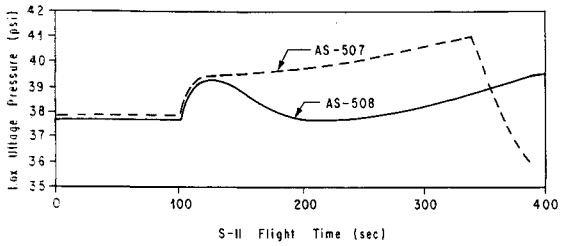

Fig. 13 Ullage pressure differences between AS-507 and AS-508.

It is usually not possible to obtain good measurements at the pump inlet. For this reason, most of the available data on the suction side of the pump have been taken some appreciable distance upstream. For this particular engine, Rocketdyne took the data 42 in. above the pump inlet, while measurements made at Marshall Space Flight Center were taken 24-in. upstream. These measurements were obtained by pulsing an engine to determine the dynamic response while operating the engine at a particular NPSH and mixture ratio (MR). These data were used to curve-fit a transfer function of the form

$$\partial F/\partial p_{os} = \frac{K(1 + s/2\pi f_1)}{(1 + s/2\pi f_2)[1 + (2\zeta s/2\pi f_3) + (s/2\pi f_3)^2]} \quad (8)$$

where the parameters K, ζ, f_1, f_2, and f_3 are functions of MR and NPSH. This equation includes the dynamics of that portion of the suction line included in the measurements. Because this effect is significant, a correction was made using the inlet impedance stiffness, stiffness and damping as determined in dynamic tests of the feedlines, and the inertia of that short section of feedline that was inadvertently included.

System Simulation

The basic equations presented thus far have been combined into a model and implemented on an analog computer simulation. A block diagram is shown in Fig. 10. The fuel loop, including the tank, suction line, engine dynamics, and cross-coupling, has been deleted. Previous analysis has shown the contribution from the fuel loop to be negligible.

The resulting system is represented by three major blocks: the structural dynamics, the oxidizer suction line dynamics, and the J-2 engine dynamics. The structure is forced at two principal points: the center engine and the four outboard engine parameters have been combined because of symmetry considerations. The oxidizer suction line is excited by flow perturbations resulting from both the pump deflections and the LOX sump pressures.

Using this total simulation with time-varying coefficients, time response analysis is made using random noise input to the thrust as a forcing function. In special cases, the noise is deleted and initial conditions are input to start the oscillations.

Results

Using the component model and over-all system model, analog time response runs were made to gain understanding

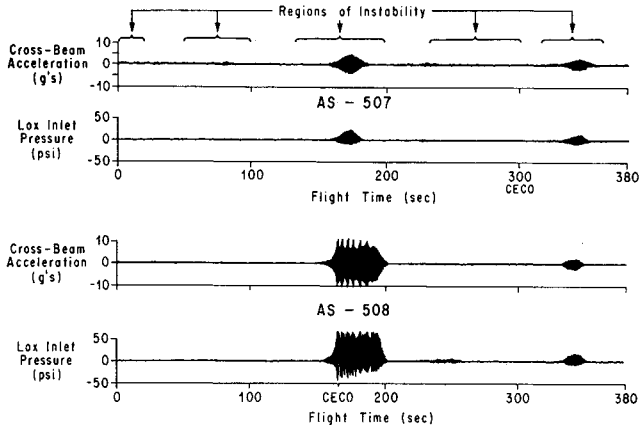

Fig. 14 S-II simulation response to noise (CECO).

of the S-II POGO phenomenon by varying the different parameters known to be important in the POGO loop.

The S-II stage uses step pressurization to attain and maintain correct operating pressure. Figure 11 illustrates the effect of both positive and negative steps in ullage pressure. A 1-g initial condition was placed on the system. For the nominal conditions the system is slightly stable and the amplitudes eventually return to zero. A 2-psi increase in ullage pressure increases stability and drives the amplitude to zero more rapidly; on the other hand, a 2-psi decrease in ullage pressure drives the system unstable. The positive pressure step adds damping to the system by shifting the operating point upward on the nonlinear spring constant curve (Fig. 8), while the negative step destabilizes the system by shifting the operating point on the nonlinear curve downward. The larger amplitudes cause the system to become strongly nonlinear and highly unstable near the end of the run.

To remove the effects of the transient of the step and time-varying coefficients, a constant coefficient case was run for various operating points on the nonlinear spring curve (NPSH variations). In Fig. 12a, the envelopes of the oscillations are shown for the cross-beam acceleration and the thrust perturbations. It is clear that increasing NPSH increases stability and vice versa. Again, this is caused by the system softening for the lower (NPSH) values and tuning more with the structural modes. Also, once the nonlinear range (amplitude) is reached, the system destabilizes rapidly.

The same effective results can be obtained by changing the amplitude of the initial conditions used to start the oscillations as shown in Fig. 12b. This change shows clearly the dependence of stability of the loop on the amplitude.

Because the assumed characteristics of the nonlinear bubble were known only qualitatively, the effects of possible changes of the slope of the spring constant curve (Fig. 8) between NPSH values of 10 and 35 were investigated. The numbers in Fig. 12c indicate the factor of change in the slope of this segment of the curve. Making the slope flatter ($K < 1$), approaching a linear spring value, has a stabilizing influence and vice versa. For the steeper curve smaller amplitudes are required to drive the line frequency toward the structural frequency, thus the system is destabilized.

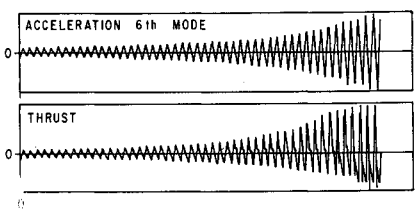

Fig. 15 Characteristics of the nonlinear response.

Figure 13 shows the differences in ullage pressure observed on two recent S-II flights (AS-507 and 508). Figure 14 is an analog response run of the two flights using the previous ullage pressure curves. The system is excited by a small random noise input into the thrust. Complete time-varying coefficients were used in this simulation. The two cases show at least a qualitative explanation of the differences observed in the AS-507 and AS-508 flights. The large oscillation occurred on AS-508, shutting off the center engine near the same point where saturation occurs on the analog computer. Since the computer was not scaled to an amplitude large enough to duplicate flight, no direct comparison can be made.

Figure 15, showing the characteristics of the oscillations, is a blow-up of one of the computer runs in a nonlinear, unstable region. The LOX pump pressure has the same characteristics observed on flights, a short upper peak with a rounding or flattening on the bottom. Also, the harmonic is shown to be shifting downward as the AS-508 flight record showed.

Conclusions

The results to date show a qualitative explanation of some of the anomalies observed in Saturn Apollo POGO oscillations. The results are not at all quantitative and do not yet explain all the characteristics seen on these flights; for example, the decaying of oscillation in AS-504 near the end of burn after the oscillation had clearly reached the highly nonlinear range. The need for many sensitivity studies and care in making any changes in system parameters are strongly indicated, as well as the need for a better understanding of the physical phenomena and thus more accurate models. Particularly are the bubble characteristics and pump characteristics in need of additional theoretical and test analyses in order to substantiate the character of the assumed nonlinearity.

References

[1] Rubin, S., "Longitudinal Instability of Liquid Rockets Due to Propulsion Feedback (POGO)," *Journal of Spacecraft and Rockets*, Vol. 3, No. 8, Aug. 1966, pp. 1188–1195.

[2] Sack, L. E. and Nottage, H. B., "System Oscillations Associated with Cavitating Inducers," *Transactions of the ASME, Journal of Basic Engineering*, Vol. 87, Ser. D, No. 2, Dec. 1965, pp. 917–924.

[3] Stripling, L. B. and Acosta, A. J., "Cavitation in Turbopumps," *Transactions of the ASME, Journal of Basic Engineering*, Vol. 84, Ser. D, No. 3, Sept. 1962, pp. 339–350.

DECEMBER 1970 J. SPACECRAFT VOL. 7, NO. 12

Hypervelocity Impact of Bumper-Protected Fuel Tanks

PEI CHI CHOU* AND SHUN CHEN†

Drexel University, Philadelphia, Pa.

The problem of the fracture of bumper-protected, liquid-filled fuel tanks subjected to hypervelocity meteoroid impact is studied. The method of characteristics in finite difference form is applied to the equations governing stress wave propagation in the tank walls. The pressure field of the debris cloud from the perforated bumper is obtained from a semiempirical formula. The reaction of the liquid fuel due to the wall motion is calculated from the shock Hugoniot of the fuel and the wall velocity. Deflections calculated from the present theory are in good agreement with experimental measurements. The deflection and stress levels in a fuel tank are found to be one order of magnitude smaller than those produced in an empty tank.

Nomenclature

a,b = constants
c_p = plate velocity = $[E/\rho_1(1-\nu^2)]^{1/2}$
c_2 = shear wave velocity = $(G/\rho_1)^{1/2}$
D = flexural rigidity = $Eh^3/12(1-\nu^2)$
E = modulus of elasticity
G = shear modulus = $E/2(1+\nu)$
h = plate thickness
k_2 = shear correction factor
M_r,M_θ = radial and tangential bending moments, respectively
P = pressure loading function
P_1 = pressure constant
P_o = pressure ahead of shock front
P_f = pressure behind shock front
Q_r = transverse shear stress resultant
r = radial distance
t = time
t_1,t_o, = time constants
U = shock front velocity
u = particle velocity of liquid behind shock front
w = transverse displacement of the midplane
z = transverse distance from midplane
β = constant
ν = Poisson's ratio
ρ = density of liquid behind shock front
ρ_1 = density of plate
ρ_o = density of liquid ahead of shock front
σ_r,σ_θ = normal stresses due to M_r and M_θ, respectively
τ_{rz} = shear stress due to Q_r
ϕ = rotation of the cross section about the tangential axis‡

Presented as Paper 69-369 at the AIAA Hypervelocity Impact Conference, Cincinnati, Ohio, April 30–May 2, 1970; submitted April 29, 1970; revision received August 3, 1970. This research is supported by NASA Lewis Research Center, under Grant NGL-39-004-001.

* Professor of Aerospace Engineering. Associate Fellow AIAA.
† Research Associate. Member AIAA.

‡ Subscripts r and t affixed to ϕ and w designate partial differentiations.